Chapter 16
Microhotplates and Integration with Metal-Oxide Nanomaterials

Emanuele Barborini

Abstract The current scenario of metal-oxide gas sensing shows, on one side, highly innovative silicon-based platforms, as outcomes of microelectronic and micromachining manufacturing processes, while on the other side, several techniques and methods for the synthesis of the metal-oxide active layers in the form of nanoporous-nanostructured coatings. The high specific surface area of nanoporous coatings improves the interaction with the atmosphere, while the nanostructure offers characteristic surface-dependent electrical properties. Changes in these electrical properties upon gas exposure and interfacial chemical reactions allow for the development of novel, nano-enhanced gas sensors. The base element of innovative micromachined platforms for gas sensing is the microhotplate. Although microhotplates have the same functional parts of traditional devices (integrated heater, electrodes for resistance readout), micromachining provides considerable improvements. These include, for example, the 2–3 orders of magnitude reduction in power consumption for heating: a feature that may disclose the possibility for remote powering through batteries or photovoltaic cells. Moreover, microhotplates originate from the manufacturing track of microelectronics, hence the concept of "system integration" turns out straightforwardly. Within this perspective, the microhotplate may be considered as just an individual component of a many-element sensing platform, including for example, other transducers, or even on-board front-end electronics. Integration concepts are also needed for optimizing the functionalization of the microhotplate with the metal-oxide nanostructured sensing layer, whose batch deposition should become one step of a device production pipeline. As two beautiful countries separated by the sea, with just few bridges in between, difficulties still exist from the point of view of the integration of metal-oxide nanomaterials on microhotplates and micromachined platforms in general. In fact, although many different

E. Barborini (✉)
Tethis spa, via Russoli 3, 20143 Milan, Italy
e-mail: emanuele.barborini@tethis-lab.com

M. A. Carpenter et al. (eds.), *Metal Oxide Nanomaterials for Chemical Sensors*, Integrated Analytical Systems, DOI: 10.1007/978-1-4614-5395-6_16,
© Springer Science+Business Media New York 2013

techniques for the production of metal-oxide nanomaterials have been developed so far, each one of them suffers difficulties, at various degrees, with respect to the fundamental step of microhotplate functionalization. For example, the high temperature step required by certain techniques for stoichiometric oxide synthesis, may be incompatible with microhotplate safety, while the mechanical stress during deposition may result in microhotplate destruction and a subsequent low production yield. The chapter will describe the concepts and the technologies behind microhotplates manufacturing with respect to drawings adopted, chosen materials, and system integration approaches. Techniques and methods for metal-oxide nanomaterial production will be reviewed, highlighting weaknesses and strength points, once they would be employed for microhotplate functionalization. Recent developments on the use of nanoparticle beams to directly deposit nanoporous coatings on microhotplate batches will be included: besides providing thermal and mechanical compatibility with microhotplates, these methods also offer the possibility to synthesize a wide group of different metal-oxides, which is beneficial for an array approach to gas sensing. Relevant examples of sensing performances of microhotplates-based devices will be reported as well.

16.1 Introduction

The phenomenon of a reversible change in electrical conduction of metal-oxides at high temperature, once exposed to airborne chemical compounds, has been known for decades, and has been exploited from the very beginning to make chemical sensors, called conductometric or chemoresistive sensors. More recently, from the middle of 90s, we are experiencing an outburst of development for novel metal-oxide gas sensing solutions, driven by the progresses within each one of the technological players composing the “sensing system team”: the electronics, required to deal with the electrical features of chemoresistive sensors; the software, in charge of sensor data analysis by means of “artificial intelligence” and advanced algorithms; and mostly the device platform and the active sensing material, constituting the transducer that detects the presence in air of chemical compounds. In fact, on one hand highly innovative silicon-based platforms became available from the union of microelectronic and micromachining manufacturing processes, while on the other hand novel methods for the synthesis of the metal-oxide active layers in the form of nanoporous coatings were introduced. The high specific surface area of nanoporous coatings provides an efficient interaction with the atmosphere, while the nanostructure determines the strongly surface-dependent electrical properties, and both characteristics lead to improved sensing performances.

Behind these technological efforts, there is the understanding that sensing systems may have pervasive applications if further improvements of issues such as miniaturization, reduced power consumption, portability, etc. as well as reliability of production pipeline, will be reached. Such advanced microsensors could

become the basic elements for the development of complex detection systems for real-world scenarios, where the heterogeneity of operative conditions, from the point of view of the chemical composition of the detection atmosphere, and of the distribution of chemical compounds in space, is a typical monitoring situation.

An example of a crowded class of applications is atmospheric monitoring by sensor networks. This includes outdoor opportunities in metropolitan air quality monitoring or in spatially resolved early detection of environmental chemical risks (either from human activities such as airborne leakage from industrial sites or chemical spills in rivers, or from natural events such as emissions from active volcanic sites). Indoor opportunities exist as well and may include domestic applications for air quality in houses, the monitoring of atmosphere within industrial buildings where processes are executed in atmosphere-controlled conditions (such as industrial agro-food production and storage), up to the monitoring of microclimatic physical-chemical conditions within cultural heritage sites to ensure optimal preservation. In all these cases what is needed is a large number of miniaturized devices and dedicated electronics, both having low-cost and low-power consumption. These systems would provide a network of sensing nodes which would be able to detect chemicals over large areas with meaningful spatial resolution.

A second example with pervasive character is within the framework of the so called artificial olfactory systems or electronic noses, where the final goal is the recognition and quantification of different compounds (or at least their chemical family) within complex mixtures. The sensing system acting as an electronic nose should be able to conciliate unspecificity, i.e. a sensitivity extended to many different chemical compounds, with selectivity, to recognize each one of them. The approach to face this task, requiring two apparently incompatible properties, is based on microsensor arrays, having many different sensing elements whose collective response is interpreted by a trained intelligent software (principal component analysis, neural networks, etc.). In this case, the integration of a suitable number of different miniaturized sensing elements on the same platform is the issue to be addressed. An electronic nose may find important applications, for example in the food industry. Specifically, these may include the rapid characterization of product freshness, proper storage, ripening degree, and geographic origin. Other challenging applications would be within the biomedical field for assisting in disease diagnosis through breath analysis.

Due to the principle of operation of metal-oxide sensors, whose electrical resistance at high temperature changes according to the presence of reactive chemical compounds within the surrounding atmosphere, the parts constituting traditional devices include: a ceramic platform, a pair of electrodes for resistance measurements on one side of the platform, the sensing metal-oxide layer across the electrodes, and an integrated heater on ceramic platform backside, as shown in Fig. 16.1.

Although the generic term “metal-oxide” is commonly used throughout this chapter, it is worth noting that the state-of-the-art in the production of metal-oxide nanostructured layers is generally limited to a few metal-oxides, namely SnO_2, WO_3, TiO_2, among a few others. However, SnO_2 is by far the species that has been

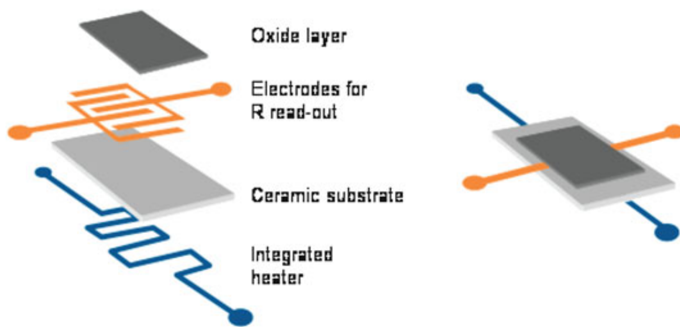

Fig. 16.1 Structure of a traditional chemical sensor based on metal-oxide sensing layer. A ceramic platform (typically alumina) has electrodes patterned on its *front-side*. The electrodes are coated with a metal oxide layer and are used for read-out of changes in the metal oxide electrical resistance. On the backside, an integrated heater provides high temperature operation

used the most. Heating power on the order of several hundreds of milliwatts is usually spent to heat up the ceramic platform to 300–400 °C, while thermal insulation is achieved by suspending the platform to bonding wires, looking for a delicate compromise between lowering thermal conduction through wires, reducing their diameter, and maintaining a sufficient wire robustness.

The base element characterizing innovative silicon-based micromachined platforms is the microhotplate: a structure constituted by a sub-millimetric sheet with a thickness of a few micrometers, hosting the electrode pair for sensor read-out and the integrated heater. Although microhotplate components implement the same functions as the parts within traditional devices (Fig. 16.1), micromachining and miniaturization provide considerable improvements. First, minimal heated area and reduced thermal contact at borders results in heating power consumption of a few tens of milliwatts (one or two order of magnitude lower than traditional platforms). This improvement opens up the potential for powering through remote sources such as batteries or photovoltaic cells. Second, the minimized thermal mass results in rapid heating and cooling times which enables modulated temperature operation mode (or temperature programmed sensing). This leads to advantages from the point of view of power consumption as well with gas selectivity exploited through the reactivity temperature dependence of the target compounds. Third, since microhotplates are manufactured using microelectronic processes, it is quite natural to address "system integration". In this framework the microhotplate is an individual component within a complex miniaturized sensing platform, having for example, other microhotplates for an array approach, or other micromachined transducers (air temperature, flow, pressure, etc.), or even on-board front-end electronics.

Unfortunately, besides these intriguing features, difficulties still exist from the point of view of the integration of active metal-oxide nanomaterials. In fact, although many different techniques for the production of metal-oxide layers have been developed so far (including either thin and thick films), each one of them, at various degrees, introduce difficulties with respect to the fundamental step of microhotplate

functionalization. These difficulties may range from high temperatures required by certain techniques for stoichiometric oxide synthesis, which are incompatible with the microhotplate components, to mechanical stresses during deposition, that may result in the destruction of the microhotplates and a low production yield. Therefore, the transition from lab-scale to market-scale of sensing technology based on microhotplates is still hampered by the lack of a reliable, cost effective, and most of all a microhotplate compatible method for large-scale integration with metal-oxide nanostructured sensing layers.

Throughout this chapter we will use the term "integration" to indicate the deposition onto micromachined platforms of the active metal-oxide layer. By adopting this term we intend to underline that the functionalization of these platforms is not a merely deposition of a thin or thick film on a flat substrate: it is one task of a sequence of complex tasks leading to the final, operative sensing device. Within this meaning the functionalization has to be carried out taking care of constraints related to other tasks, and synergistically with them.

Besides the *Introduction* and the *Conclusions-Perspectives*, the contents of this Chapter are arranged into the following sections.

Microhotplates and Micromachined Platforms, where the technology behind microhotplates and micromachined platforms manufacturing will be reviewed with respect to drawings adopted, chosen materials, and system integration.

Nanomaterials Integration/Functionalization Methods, where deposition methods will be addressed, pointing out, among different deposition techniques, advantages and disadvantages once they would be employed for microhotplate functionalization. Recent developments on the use of nanoparticle beams to directly deposit nanoporous coatings on microhotplate batches will be included: besides providing thermal and mechanical compatibility with microhotplate, these methods also offer the possibility to synthesize a wide group of different oxides, which is beneficial for an array approach to chemical sensing.

Sensing Performances, that will show the most relevant characteristics of microhotplates-based chemical sensors

16.2 Microhotplates and Micromachined Platforms

16.2.1 Basic Structure Description

Many different designs of microhotplates have been developed so far, however, their general structure is the same: a thin sheet of silicon oxide or nitride, which is suspended within a bulky silicon frame (for this reason microhotplates are also called "suspended silicon membranes"). Above this sheet, all the elements required for sensor operations are stacked in a multi-layered configuration. These include the sensing layer, the electrode pair for the read-out of the sensing layer resistance, a thermometer, and a suitable heater. Passivation layers provide electrical insulation

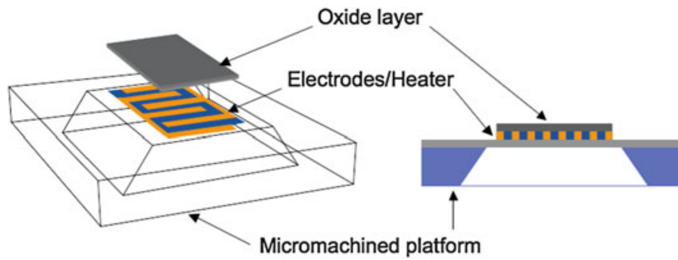

Fig. 16.2 Schematic of a microhotplate-based chemical sensor. Functional elements described in Fig. 16.1, namely the oxide layer, the electrodes and the heater, are also present within this type of devices (for simplicity, thermometer and passivation layers are omitted). Microelectronic techniques are adopted for the creation of the functional elements, while micromachining techniques are adopted to obtain the miniature base sustaining them. Typical dimensions of a microhotplate are sub-millimetric

between the heater, thermometer, and the sensing layer. Figure 16.2 schematically shows the structure of a microhotplate-based chemical sensor.

Due to the minimal thermal contact at the border along with the minimal heated area (resulting in a minimal contact, convective and radiative heat transfer) a microhotplate is able to reach temperatures up to 300–400 °C with a power consumption of the order of a few tens of milliwatts. The integrated heater typically has a serpentine-like shape, to ensure uniform heating. Microhotplate temperature may be estimated by means of the resistance of a dedicated metal film, acting as a thermometer, which is located between the heater and the sensing layer. If proper characterization of the heater is available, the measure of its resistance by suitable electronics could also be used for temperature evaluation, avoiding the use of a dedicated thermometric element (and simplifying manufacturing). A useful configuration of the electrode pair is the so called interdigitated one, where electrodes look like a pair of many-fingered hands co-penetrating each other, as visible in Fig. 16.2.

Microhotplate manufacturing exploits a microelectronic-like process and a micromachining process, using silicon wafers as the substrate. The first one, sometimes addressed as CMOS-like process (see below), regards the production of the functional elements described above—heater, thermometer, electrodes, and passivation layers. While the second one regards the chemical etching of bulk silicon in order to remove material and generate the final micrometer-thick membrane. The union of microelectronic and micromachining processes leads to the possibility of creating complex 3D structured devices generically called MEMS (micro-electro-mechanical systems), of which microhotplates are a paradigmatic example. We will see in the following some examples of microhotplate-hosting systems, where the device structure has been tailored by micromachining processes to address particular requirements. Specifically, these include having a variety of transducers on the same platform, or providing a temperature-array chemical sensor to exploit the temperature dependent chemical reactivity of different target compounds.

16.2.2 Manufacturing Route

Figure 16.3 reports the step sequence for manufacturing a microhotplate starting from a silicon wafer. Details may be found in several references such as, for example, refs. [1–3] and those therein. It is worth to note that these steps are very similar to those currently used in the microelectronic industry for microchip manufacturing.

Before describing the method and the steps to create the functional elements on the front-side of the microhotplate, it is necessary to anticipate now a concept related to the micromachining step, the last one of the manufacturing route. Bulk silicon removal is performed by chemical etching in liquid-phase by means of potassium hydroxide (KOH) or ethylenediamine and pyrocatechol in aqueous solution (EDP), at the end of front-side manufacturing. Etching is carried out on the wafer backside and removes as much bulk silicon as to preserve a micrometer-thick sheet having functional elements already created on it. The precise control of the chemical etching process is based on the knowledge that silicon oxide or silicon nitride cannot be removed by either KOH or EDP.

The first step of front-side manufacturing is therefore the oxidation (or nitridification) of a suitable layer of silicon wafer, as shown in Fig. 16.3, that will serve as the stop for chemical etching from the back-side. In addition, silicon oxide and silicon nitride possess a low thermal conductivity (1.4 and 9–30 $Wm^{-1}K^{-1}$ at 300 K, respectively [4]), a benefit for thermal insulation of the final structure. Although differences do exist, subsequent steps may be considered as standard steps of CMOS-like microelectronic production: a sequence of photolithography, thin film deposition and lift-off steps, leading to the formation of the multi-layered top structures (heater, thermometer, electrodes, and passivation layers).

One of the differences with respect to standard CMOS processes used in microelectronics is the metal to be used for heater, thermometer, and electrodes, which is usually platinum. Metallization for standard CMOS processs uses aluminum, nevertheless its limited thermal stability, causing either oxidation and atom diffusion at temperatures around 500 °C, prevents its use in microhotplates. As a noble metal, platinum offers much larger thermal stability than aluminum, it can be easily deposited, by sputtering or evaporation, and patterned by lift-off. Due to the linear behavior of resistance versus temperature, according to $R_T = R_0 \cdot (1 + TCR \cdot \Delta T)$, where R_0 is the resistance value at room temperature, R_T is the value at high temperature, TCR is the temperature coefficient of resistance, and ΔT is the temperature difference, platinum can be effectively used as material for integrated thermometric measurements. Typical TCR values of platinum are around 2×10^{-3} K^{-1}.

An alternative to platinum heaters is poly-crystalline silicon (polysilicon) heater, which can be introduced into the CMOS process in straightforward way, as it requires standard low-pressure chemical vapor deposition (LPCVD) as a deposition method, and standard photolithography for patterning. An advantage of polysilicon is the possibility of resistivity tuning by n-type phosphor doping, using $POCl_3$. Although much variable, TCR values of polysilicon are commonly around 0.5×10^{-3} K^{-1}.

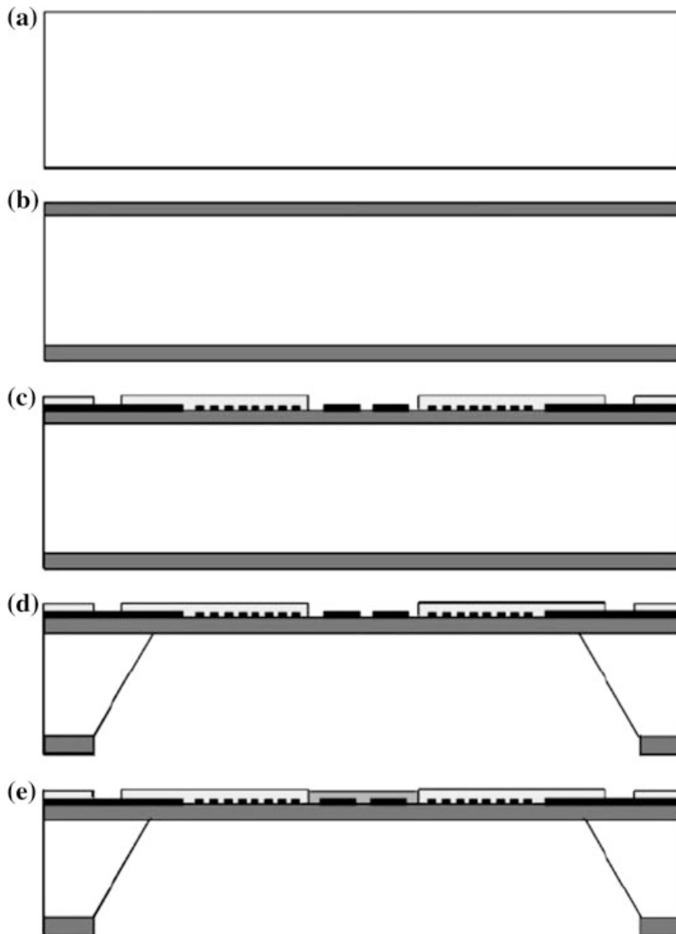

Fig. 16.3 Process steps for the production of a microhotplate starting from a silicon wafer: **a** silicon wafer with about 0.4 mm thickness; **b** dielectric layer deposition (SiO_2 or Si_3N_4); **c** deposition of metals for electrodes and heater (*black* parts), and of silicon oxide or nitride for passivation (*light grey* parts); **d** backside anisotropic etching by KOH; **e** deposition of active metal-oxide layer. Reprinted from Ref. [1] with permission from Elsevier

Electrodes for the read-out of the sensing layer resistance may be planar or interdigitated. Since metal-oxide nanostructured layers typically show very high resistance values (reaching hundreds of megaohms and more), the peculiar drawing of interdigitated electrodes has the advantage of facilitating the resistance measurements, with respect to simple planar electrodes, decreasing the read value by means of a purely geometrical argument. Referring to Ohm's 2nd law and to Fig. 16.4, the resistance of a square ideal conductor as measured by planar electrodes is $R = \rho \frac{1}{th}$ (where ρ is the material resistivity and th is the conductor

Fig. 16.4 The read-out of the resistance of metal-oxide layers may be hampered by its extremely high values. For a given area of active material, it turns out, by geometrical arguments, that interdigitated electrodes (*right*) are more effective than planar ones (*left*)

thickness) while in the case of interdigitated electrodes, resistance of the same conductor is $R \approx \rho \frac{1}{(2 \times N)^2 th}$ (where N is the number of fingers in one electrode). The factor, $(2 \times N)^2$ results in a considerable decrease in measured resistance.

To electrically separate the three circuits for the heater, thermometer, and electrodes for sensing layer read-out, silicon oxide layers are deposited between each metallization by CVD, at a thickness typically not larger than 0.5 μm. Silicon nitride deposited by CVD (for example from ammonia and dichlorosilane) can alternatively be used for the same purpose.

When functional structures on the front-side are completed, the wafer undergoes micromachining through back-side chemical etching. Exploiting the phenomenon of anisotropic chemical etching, where the etching rate of a crystalline material depends on the crystal face exposed to the etchant, a pyramid-like pit is created, starting from the wafer backside and moving toward its front-side. Once the etching front reaches the silicon oxide (or nitride) layer, it stops. This results in the final structure having a trapezoidal cross section as shown in Figs. 16.2 and 16.3. The ratio between the etched thickness and the enlargement of the etched region with respect to final size of the suspended part is related to the anisotropy of etching rates, that is the ratio between normal-to-plane and in-plane etching rates. If structures with a higher aspect-ratio need to be produced, wet chemical etching has to be replaced by plasma etching.

Backside etching has the capability to create structures having thicknesses as small as 1–2 μm, nevertheless it has the drawback of being a double-sided process, making mask alignment more difficult than one-sided standard lithography, as usually done in microelectronics. To overcome this limitation front-side chemical etching can be introduced. An additional photolithographic step on the wafer front-side leaves four unprotected areas (etch windows) beside each of the microhotplate sides [5], as shown in Fig. 16.5. Front-side etching removes silicon from unprotected areas, starting from the front-side and moving under the central area hosting the functional structures. Once the etching step is concluded, the microhotplate will stay suspended by means of suitable beams over a closed pit etched into the bulk silicon. Backside etched microhotplates have typical dimensions between 1×1 and 2×2 mm^2, while front-side etched ones may be quite smaller (0.2×0.2 mm^2).

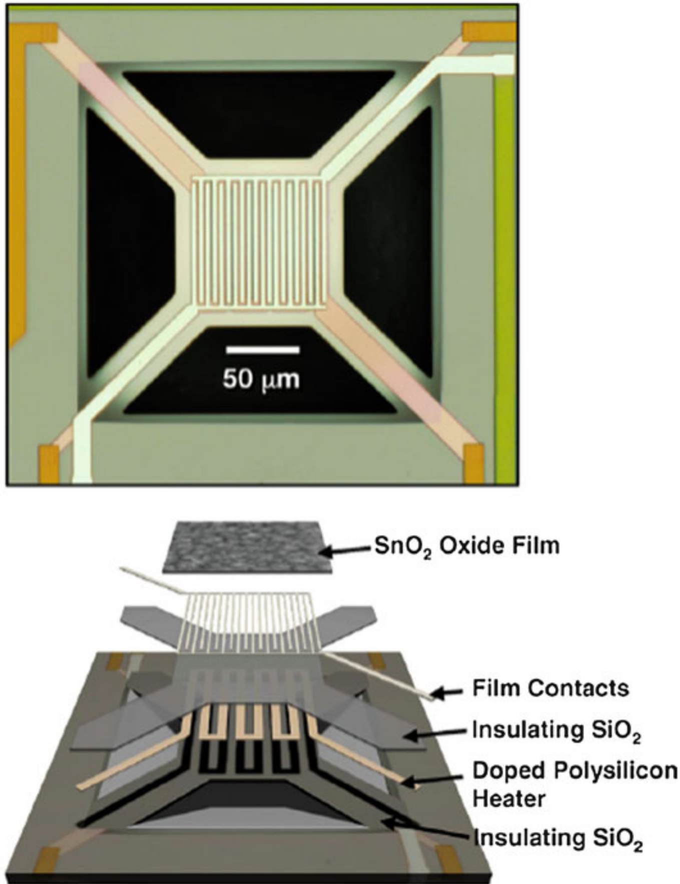

Fig. 16.5 Optical micrograph showing an example of a suspended membrane (*top*), and a lift-away scheme showing the functional elements composing the device (*bottom*). Reprinted from Ref. [5] with permission from Elsevier

Since so many details addressing each one of the manufacturing steps, from metallization to passivation, from wet etching to plasma etching, are reported in the technical literature, the general feeling a reader may have is that a large degree of freedom and space for novel experimental approaches exist on this matter. This also holds for the implemented geometries, such as the shape of the heater or that of electrodes, up to the general structure of the devices.

16.2.3 Advanced Structures

From the point of view of system integration, microhotplates could be considered as the first building block in the development of advanced platforms for sensing, based on the integration of various transducers. For example, several microhotplates could be arranged into the same platform exploiting an array approach to sensing; a microhotplate could be machined side by side with physical transducers (temperature, pressure, flow), on the same silicon platform, for hybrid physical-chemical microsensors; the silicon platform hosting the microhotplate could also host CMOS front-end electronics for impedance matching, signal pre-amplification, and data analysis.

One of the drivers for the creation of complex platforms resides in the possibility to increase the amount of simultaneously collected data, with spatial resolution, improving our capabilities to face the challenging task of physical-chemical characterization of atmospheres. An array of chemical sensors in fact generates many signals qualitatively similar each other, although not identical. By exploiting this collective output, it could be possible to associate a certain atmosphere to a certain signal fingerprint. An array-based approach to face complex scenarios requires to pass through a training step where advanced software is needed to determine the correlations among a known atmosphere composition and the array collective output. Once training is completed and correlations identified, the system should be ready not only to recognize the atmospheres seen during training, but to perform a certain degree of "extrapolation" to identify unknown atmospheres. While we do not cover this subject in this chapter, the reader is referred to other chapters within this text. Regardless, the starting point to deal with many-signals is the availability of suitable array-like platforms.

A first example of a sensor array platform is a microhotplate where the heater has been designed in a suitable way to generate a temperature gradient under a multi-electrode pattern [6], as shown in Fig. 16.6. Although this is still a single microhotplate, and will be functionalized with the same metal-oxide layer, the combination of multi-electrodes and a temperature gradient allows the read-out of portions of the active layer operating at different temperatures. This produces a sensor array which utilizes the temperature dependent reactivity of gases, to provide a multi-signal output.

A second example of multi-signal sensor array platform is a true microhotplates array, where the microhotplate structure is replicated many times on the same device [3, 7], as shown in Fig. 16.7. Operation at different temperatures can be pursued also in this case, nevertheless this setup is particularly suited to using different metal-oxides as sensing layers. Since it is not trivial at all to be able to produce and integrate on this kind of platforms many different metal-oxides, a commonly adopted approach is doping. In this case, the different sensing elements are obtained through the introduction of different noble metals into the same metal-oxide, which is typically tin oxide [8–10]. This configuration is a "material

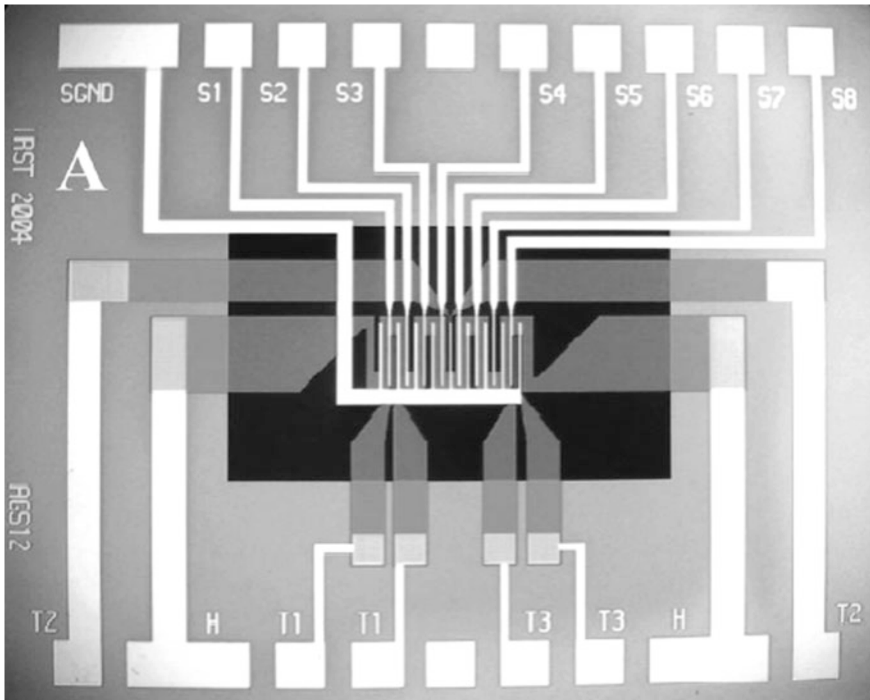

Fig. 16.6 Example of a micromachined platform where the heater (horizontal serpentine pattern in the center of the image) has been manufactured in order to generate a temperature gradient. A multi-electrodes pattern (white interdigitated structures) collects multiple signals from the same sensing material operating at different temperatures. Reprinted from Ref. [6] with permission from Elsevier

array", exploiting the different surface chemistry of gases with respect to different oxides (or different dopants), to generate a multi-signal output.

Physical sensing transducers can also be miniaturized through micromachining. Hence, beyond bare chemical sensing, micromachining techniques allow for the integration on the same platform of both chemical and physical transducers such as temperature, air flow, and pressure, to yield a multiparametric sensor. For example air flow monitoring by "hot-wire anemometry" can be performed with the micro-hotplate approach. In this case a central heater has at its sides, along the direction of the flow to be measured, two platinum thermometers; in the absence of air flow the temperature measured at the heater sides is the same; once air starts flowing a temperature mismatch between thermometers on the heater sides is revealed. Figure 16.8 (top) shows a multi-transducer platform hosting, besides the chemical sensor, a thermometer, and a micromachined hot-wire anemometer, where backside etched microhotplates are used for both the former and the latter. Figure 16.8 (bottom) shows the same kind of multiparametric platform, where micromachined

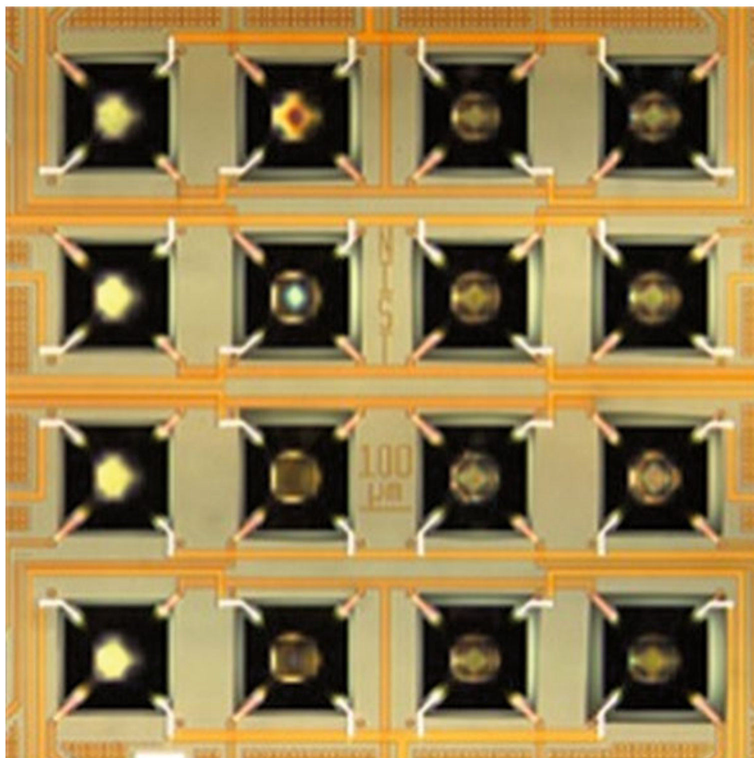

Fig. 16.7 Array of microhotplates on the same device platform. Each single element has the structure shown in Fig. 16.5, and is individually addressable and controlled in temperature. Reprinted from Ref. [7] with permission from Elsevier

structures of either the chemical sensor and the anemometer were obtained by front-side anisotropic etching, generating suspended "microbridges".

The last example of advanced sensing platforms achieved through system integration processes regards devices having on-board electronics (see Fig. 16.9 of next Section). By exploiting the affinity of micromachining methods for microhotplates manufacturing with CMOS methods for microelectronics production, the same silicon platform may host the transducers for chemical sensing, the analogical front-end electronics for signal pre-amplification, as well as the digital electronics for data pre-analysis [11, 12]. The technological driver for these efforts relies on signal handling, which gain strong benefits with respect to noise reduction if connections between transducers and front-end electronics are kept as short as possible. A second technological driver deals with the possibility to distribute at least part of the data analysis, in the case of multi-device networks.

Unfortunately, with the increased platform complexity, comes an increase in the challenges for integration of metal-oxide nanomaterials on chemical sensing areas. This means for example, that some of the deposition methods may be

difficult or impossible to adopt, or—more generally—that production yield could dramatically drop due to device damage during the manufacturing pipeline.

16.3 Nanomaterial Integration/Functionalization Methods

16.3.1 General Issues

The pipeline leading to operative sensing devices is a sequence of steps, namely: (1) CMOS-like processes for front-side manufacturing; (2) backside (or front-side) micromachining of suspended parts by chemical etching; (3) integration of active metal-oxide nanomaterial; (4) wafer dicing, bonding and packaging. This Section addresses the integration step, with the aim to give the reader a framework of the most important methods for metal-oxide nanomaterial deposition on microhotplates. It is worth to underline that many approaches that have adopted so far, each has their own strengths and its weaknesses. For this reason a well established and reliable route for the production of microhotplates-based gas sensors is still lacking and several approaches for functionalization are being developed and optimized. Within this competition, many elements have to be considered, from the level of compatibility with microhotplate characteristics to scalability for large-scale batch deposition, from batch-to-batch reliability to versatility in the synthesis of many different metal-oxides.

Concerning this last point, it has to be noted that the metal-oxide that is most widely used is by far SnO_2; oxides such as TiO_2, WO_3, ZnO, In_2O_3 also play a certain role in gas sensing, while others have just a marginal one. As anticipated, a commonly adopted way to extend the number of sensing materials is the use of various concentrations of noble metals (Au, Pt, Pd) as "dopants" or surface catalysts of the above oxides.

In general, the three most important features of a microhotplate to be taken into account to tailor the use of a certain deposition technique for metal-oxide layer integration are: (1) mechanical delicacy, (2) limited temperature of overall thermal treatments, and (3) the need for patterning. We already put emphasis on mechanical delicacy of MEMS, and microhotplates in particular. For this reason we are forced to exclude any deposition technique requiring mechanical contact with the suspended parts, otherwise this would frequently result in microhotplate damage, i.e. device damage, and unacceptably low production yield. Some integration techniques may require a post-deposition high temperature calcination step to complete the synthesis of the metal-oxide, and this may be incompatible with the preservation of front-side metallization. Particularly in complex, many-element platforms, the deposition of metal-oxide layer has to be spatially limited, i.e. patterned, to the region of heater and read-out electrodes, avoiding the contamination of other parts within the platform (other transducers, on-board electronics, etc.).

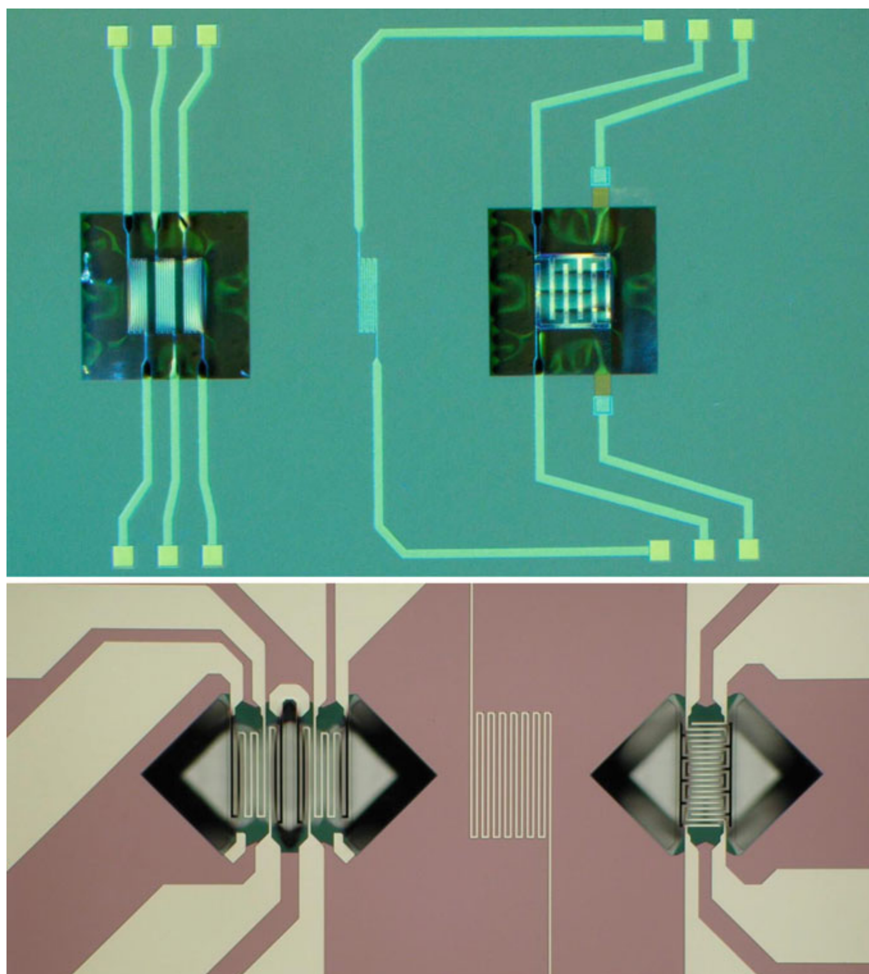

Fig. 16.8 Examples of multiparametric platforms hosting, from *left* to *right*, a micromachined hot-wire anemometer, a thermometer, and a chemical sensor. In *top platform*, backside etched microhotplates are used for anemometer and chemical sensor (courtesy from M. Lozano, CNM-Barcelona). In *bottom platform*, front-side etching was adopted, generating suspended micro-bridges (courtesy from L. Lorenzelli, FBK-Trento). In both cases the size of the entire platform is around 3×5 mm^2

Even if the step sequence reported at the beginning of this section is the most common one, alternatives do exist, where the order of the steps is modified. For example, the metal-oxide deposition step could be performed before micromachining to overcome membrane mechanical delicacy. Nevertheless, this approach imposes the need to properly protect the active layer during the subsequent etching step. As another example, last step dicing-bonding-packaging may be anticipated before metal-oxide integration. This allows for electrical connection of the

microhotplate during deposition and in this way, one can exploit the selective deposition on the heated parts occurring via reactive sputtering, a precise material patterning onto the dedicated part of a microhotplate array is achievable by switching-on the desired heater [3, 13] Although this approach may be quite useful at the research level, in the case of complex arrays, it suffers scale-up limits once batch deposition is required for large-scale production, due to difficulties in making electrical connections of all the microhotplates within a given process batch.

Concerning the integration step itself, no matter where it is located within the sequence of manufacturing steps, it turns out from the literature that borders between the characteristics of various deposition techniques, methods, and approaches are often shaded, and overlapping between topics may frequently occur. Accordingly within the structure of this chapter, the following deposition techniques have been divided between those based on wet-chemistry methods and those based on gas-phase, or physical, methods. Among gas-phase methods, a novel approach to microhotplate functionalization based on the deposition of nanoparticle beam will be also presented.

As a rough overview, generally speaking gas-phase methods lead to thin films (below some hundreds of nm), while wet-chemistry methods more commonly lead to thick films (from a few to several tens of μm); the former generate compact films, the latter porous ones. Gas-phase methods offer scale-up possibility through parallel functionalization in batch depositions. Attributes of this method include the need for patterning, the compatibility with the mechanical characteristics of the microhotplates, and the possibility of high production yields. Gas-phase methods also require an expensive vacuum apparatus and hardware. Nevertheless these setups are quite similar to systems already in use in microelectronic industry, where microhotplates come from, and their introduction within the manufacturing process is therefore not so incompatible. Wet-chemistry methods such as drop coating are serial, do not require patterning since droplets containing film precursors are dispensed one by one on the desired position. On the contrary, wet-chemistry methods such as spin coating lead to parallel functionalization and do require patterning. In both cases—drop coating and spin coating—they are not mechanically safe for microhotplates, hence technological solutions providing particular care, or a manufacturing process having micromachining after deposition are required. Although wet-chemistry methods require cheap instrumentation, hardware, and chemicals, their approach is quite far from techniques commonly used within microelectronic manufacturing, raising compatibility issues with respect to the introduction of such a step into the clean-room grade manufacturing process of microhotplates.

The general issue of functional nanomaterial integration with micromachined platforms and systems—the so called Nano-on-Micro issue—is generating new visions, where system integration concepts are driven well beyond current "microelectronic meaning", up to cover the synergistic interaction of processes and methods leading to the production of complex devices, as it will be illustrated in the following.

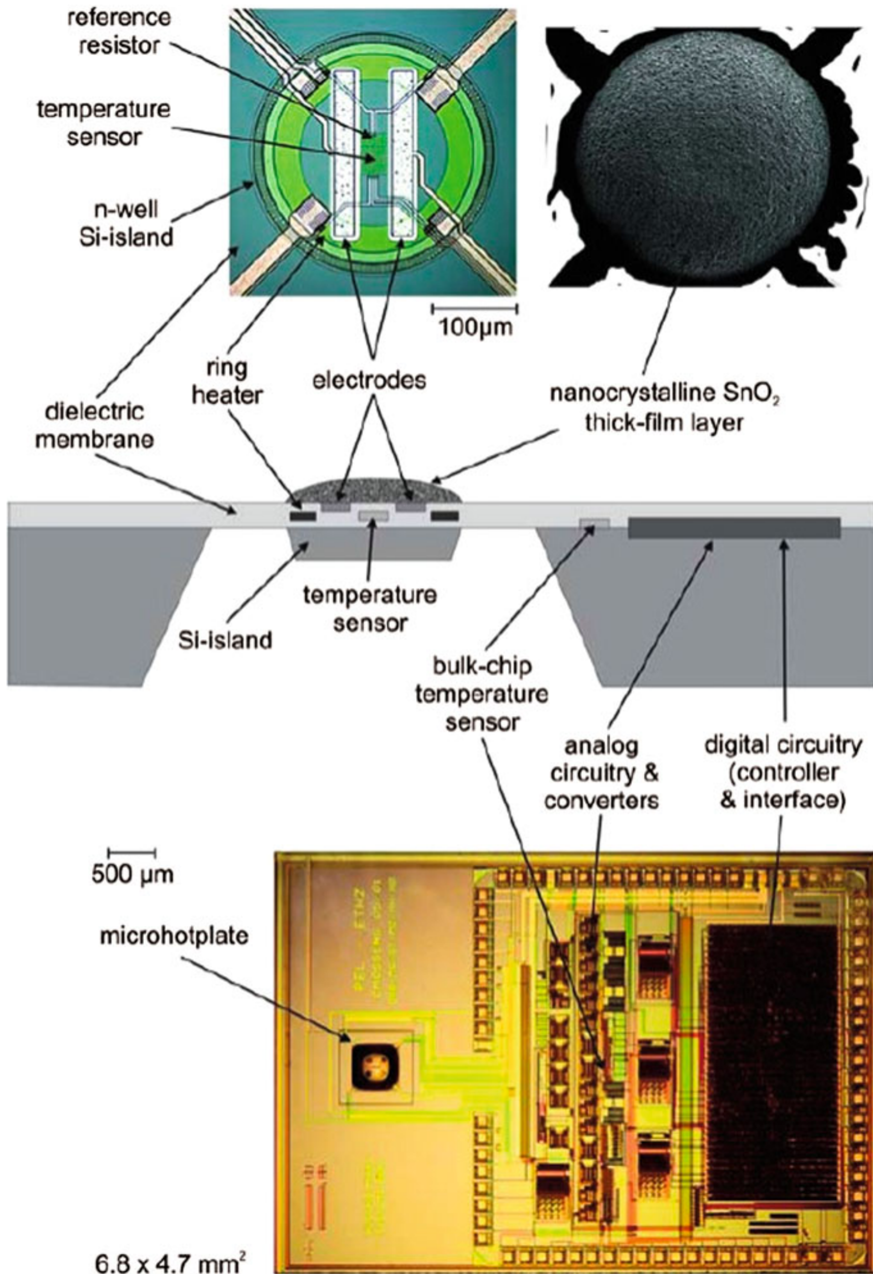

Fig. 16.9 High complexity micromachined platform for chemical sensing hosting on-board electronics. On *top*, details of the microhotplate and sensing material, which has been integrated on the microhotplate by drop coating; in the *middle*, device cross-section; on *bottom*, micrograph of the CMOS-based overall sensor system chip featuring microhotplates and circuitry. Reprinted from Ref. [14] with permission from Springer

16.3.2 Wet-Chemistry Methods

Wet-chemistry methods include various approaches to the synthesis of metal-oxide nanomaterials, namely spin coating, drop coating, dip coating, screen printing, etc., as clearly schematized in ref. [14]. In each one of these approaches, a liquid-phase or paste-form precursor of metal-oxide is added to sensor platforms in form of droplets, or in form of a continuum layer by dropping, spinning, or dipping. Advantages and drawbacks of wet-chemistry methods with respect to microhotplates integration will be highlighted below.

Starting from an initial common step consisting in the preparation of a stable suspension of a suitable precursor of the metal-oxide, two main routes can be detailed. One route passes first through the preparation of a sol-gel, then through the deposition/dropping onto the sensor platform, and finally through a post-deposition annealing step at high temperature, transforming the sol-gel into stable metal-oxide nanoparticle film (calcination). The other route, instead of creating a sol-gel from an initial suspension, anticipates the calcination step: this results in a stoichiometric and stable metal-oxide nanopowder that undergoes subsequent re-suspension into a liquid solution or into a viscous paste, and finally deposition/dropping onto the sensor platform. The difference between these routes is where the calcination step is carried out: in the latter case it belongs to paste preparation before integration onto devices, while in the former case it has to be done on microhotplates. As we already have discussed, sensing platforms may host, besides microhotplates, other components (CMOS electronic circuitry, for example) which may be incompatible with the high temperature thermal treatment required for calcination. Therefore the only way to complete nanomaterial preparation passes through the use of the integrated heater. If this is the case, not only microhotplate structure has to be as robust as it is required to survive a calcination step exploiting integrated heater temperatures of 500 °C and above, but also dicing-bonding-packaging step has to be concluded to allow the connection of the device with heater power circuitry. This “firing” step could be done at the level of manufacturing or by end users. Nevertheless, since it may deeply affect the performance of the final device, firing has to be done in well controlled and reliable conditions. Here we touch the real meaning of the “integration” concept: if a certain method for nanomaterial deposition is chosen, a certain manufacturing route in device production has to be followed.

Among wet-chemistry approaches, drop coating is the only one definitely skipping the problem of patterning: droplets with suitable size of liquid-phase precursor may be dispensed exactly onto the read-out electrodes, by means of micropipettes or microinjectors, also in the case of highly complex platforms, as shown in Fig. 16.9.

Once drop coating onto the microhotplate wafer is completed, the manufacturing route proceeds with subsequent dicing-bonding-packaging step; depending on the nature of the deposited precursor (sol-gel or calcinated paste), the additional firing step could be required or not.

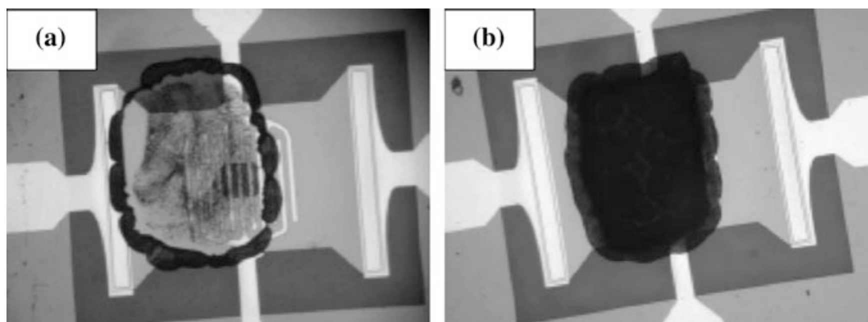

Fig. 16.10 **a** Difficulties in positioning and adhesion of metal-oxide layer by screen printing (SnO_2 thick film with size of $350 \times 500\ \mu m^2$). **b** Result improvement by proper paste formulation. Reprinted from Ref. [19] with permission from Elsevier

Drawbacks of drop coating approach regard mechanical delicacy and reliability of the electrical and sensing characteristics of metal-oxide nanomaterial. The issue of mechanical delicacy concerns the way the droplets are delivered onto microhotplates: although technologically resolvable (think about the evolution of ink jet printing heads) this operation is intrinsically critical and may result in low production yield due to high rate of microhotplates damage. The issue of reliability of electrical/sensing characteristics originates from the serial nature of drop coating, where droplets are delivered one-by-one. Paste—or suspension—itself and deposition method are required to maintain stable characteristics during the whole deposition step: events such as agglomeration, precipitation, or progressive clogging of the dispensing system have to be avoided.

The nanotech evolution of drop coating is dip-pen nanolithography (DPN) [15]. It is based on the use of the tip of an atomic force microscope (AFM) to deliver a minimal amount of a suitable “ink”, containing the metal-oxide precursor. Although limited so far to research labs, DPN could be used for extreme miniaturization of devices, avoiding any patterning procedures, and fulfilling safe conditions for microhotplates survival.

Even if literature reports successful examples [14, 16–19], other wet-chemistry approaches beside drop coating (from spin coating to screen printing) are still substantially unusable for microhotplate functionalization, due to the lacking of a safe and reliable method for patterning. Both contact hard mask and photolithographic soft mask methods in fact are difficult to implement, the former for mechanical reasons, the latter for chemical ones. Chemical incompatibilities arise due to the precursor solvents that may react with the polymeric resist of the soft mask. Likewise photoresist removal may result in damage or contamination of the sensing layer. For example, Fig. 16.10 shows difficulties in positioning and adhesion of metal-oxide layer by screen printing, and how results can be improved by proper paste formulation [19].

A completely different situation takes place if integration of metal-oxide nanomaterials is introduced before the chemical etching step for the formation of

suspended structures, as shown for example in refs. [20, 21] Although such an approach is hampered by the necessity to have a wet-chemistry step between manufacturing of front-side structures and the micromachining step, it completely rules out any difficulty related to delicacy of suspended parts. Therefore, patterning by hard mask method is no longer an issue. On the contrary, patterning may still be a problem in the case of soft masks, for chemical incompatibilities that may exist between the photoresist and the precursor solution. Efforts trying to overcome this point are reported for example in ref. [22].

Once the nanomaterial has been deposited, backside micromachining by chemical etching has to be performed, which will require the proper protection of front-side active layer with respect to etching itself and for minimization of contamination.

16.3.3 Gas-Phase Methods

Gas-phase, or physical, methods include all standard methods for thin film deposition, namely vacuum evaporation, sputtering, pulsed laser deposition (PLD), physical as well as chemical vapor deposition (PVD-CVD). Here we do not deeply describe these techniques, whose details may be found in several publications and handbooks, such as for example refs. [23–26]. We will recall the general characteristics of the techniques and show how they could match requirements for integration of nanomaterials onto microhotplates. In contrast to wet-chemistry methods, the combination of gas-phase methods, such as vacuum evaporation or sputtering, with photolithography are standard approaches used within microelectronic manufacturing. It turns out that the introduction, somewhere along the manufacturing route, of a gas-phase step for nanomaterial integration appears to be much more natural than a wet-chemistry step. Scale-up through batch processing of wafers can also be easily addressed.

Unfortunately for gas sensing applications, gas-phase deposition methods typically produce compact thin films, where the specific surface area is by far smaller than in the case of nanomaterials. It is however, possible, for the skilled person, to properly operate deposition systems and adopt procedures to generate gas-phase nanoparticles to be used as film building blocks, or alternatively, to induce suitable growth dynamics, both leading to high-roughness high specific surface area films.

Gas-phase methods are in themselves mechanically safe with respect to microhotplate delicacy, nevertheless the issue of how to pattern the deposition has to be addressed. Gas-phase deposition methods in fact are characterized by almost isotropic diffusion of film precursors, or at least by precursor trajectories within very large solid angles (as it happens in vacuum evaporators or PLD). To effectively prevent precursor diffusion and deposition onto unwanted regions, contact masks, either hard or soft, should be used. Unfortunately this is particularly challenging, if not inapplicable, on micromachined wafers. Referring to the step sequence for device production, it turns out that the use of gas-phase methods for

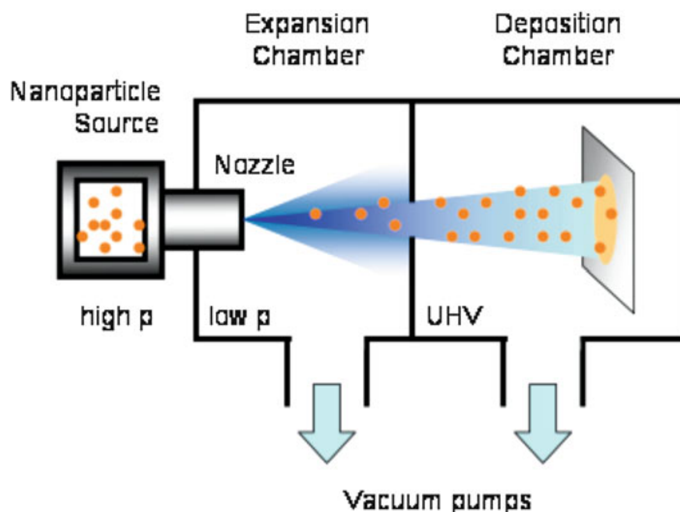

Fig. 16.11 Scheme of an apparatus for nanoparticle beam deposition. It consists of a two chamber vacuum system, where nanoparticles move from the source to deposition substrate. Once generated, for example by pulsed microplasma cluster source (*PMCS*), nanoparticles are carried by a supersonic inert gas jet expanding out of the source into the expansion chamber. The nanoparticle kinetic energy is of the order of few tenth of eV per atom: this prevents fragmentation at the impact with the substrate and allows for the soft assembly of nanoparticles, giving as a final result a nanoporous film with high specific surface area

nanomaterial integration requires some rearrangements. This could occur in two, equally challenging directions.

First, nanomaterial integration is anticipated with respect to micromachining step: as commented for wet-chemistry approaches, this definitely alleviates the microhotplate delicacy issue. Patterned functionalization of the wafer front-side may pass through standard photolithographic soft mask methods followed by lift-off, if deposition temperature is limited to photoresist-compatible values. Due to the absence of any solvent in gas-phase deposition methods, the use of photolithographic polymer soft mask is more affordable than in the case of wet-chemistry. After nanomaterial deposition, a suitable protection of the active layer against subsequent etching step has to be provided, in particular for prevention of contamination.

A second way can be followed and is based on shifting of the integration step to occur at the end on the manufacturing route, after the dicing-bonding-packaging step. By means of electrical connection to external power, integrated heaters of devices to be functionalized can be switched-on within the deposition chamber. This enables for the use of the so called self-lithographic approach, or thermally-activated CVD (it can even be applied to radiofrequency sputtering too). Self-lithography is based on the phenomenon according to which a deposition of thin film may occur from suitable precursors if the substrate is kept at a characteristic high temperature [13, 27, 28]. If the self-lithographic approach is adopted, batch

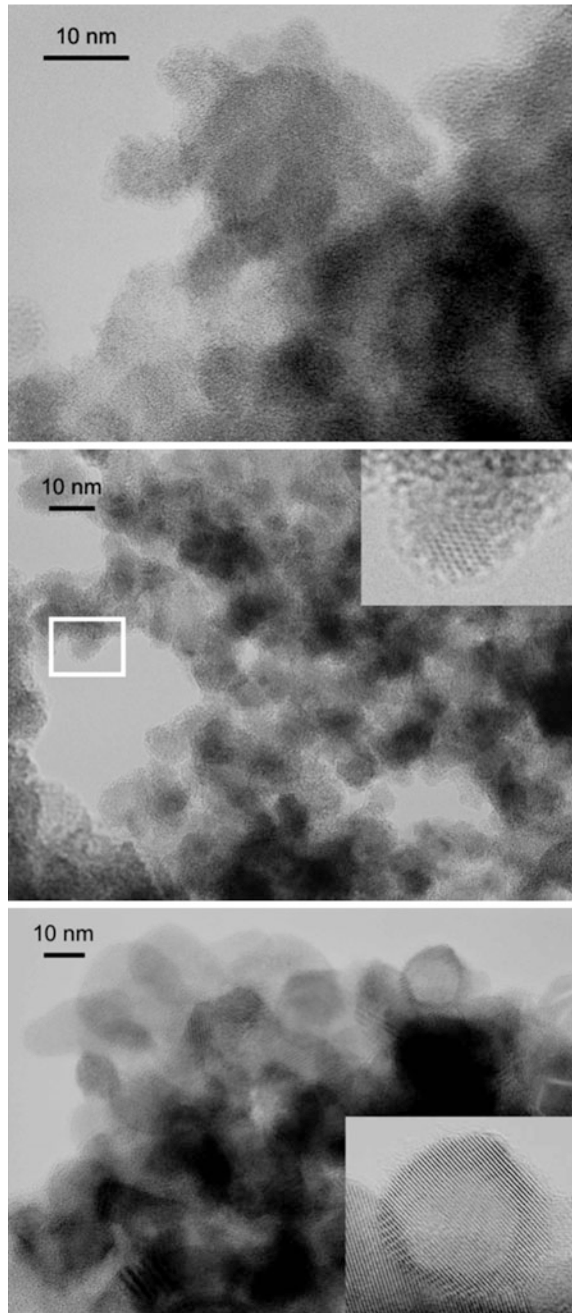

Fig. 16.12 Transmission electron microscopy (*TEM*) images of nanostructured tungsten oxide showing the structure of a film produced by nanoparticle beam deposition and the effect of thermal treatments. The as-deposited material (*top*) shows a porous structure resulting from the assembly of nanoparticles having an average size below 10 nm. The absence of lattice fringes inside the nanoparticles indicates an amorphous structure. In the 200 °C annealed material (*middle*), evolution towards a crystalline structure is evident, while the average size and porous structure are substantially identical to the as-deposited film. In the 400 °C annealed sample (*bottom*), the ordered phase fraction further increases, while maintaining the porous structure. Reprinted from Ref. [31]

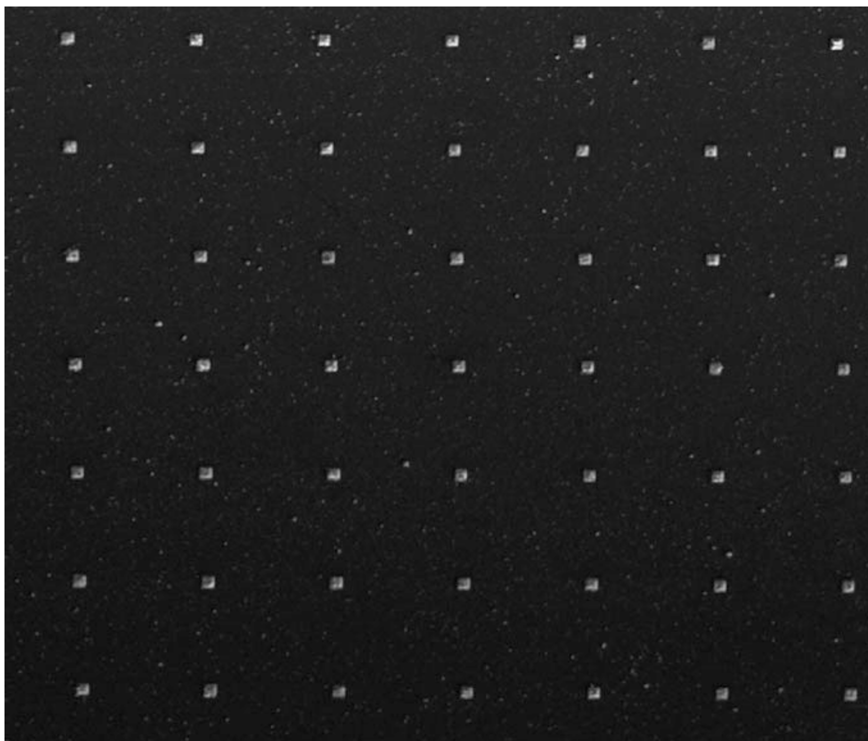

Fig. 16.13 Example of micrometric pattern of nanomaterial produced using nanoparticle beams and a non-contact hard mask. The scanning electron microscope (*SEM*) image is of a nanostructured WO_3 pattern obtained with a high-aspect-ratio micromachined silicon mask coupled to nanoparticle beam deposition system. The *dot side* is 5 μm. Reprinted from Ref. [31]

deposition on wafers is obviously no more possible since devices are separated. Even if some suitable complex wiring setup located into the deposition chamber could be imagined, the scale-up possibilities of this approach still remain quite limited.

16.3.4 Nanoparticle Beam Methods

Recently, novel gas-phase deposition techniques for the production of nanostructured films based on nanoparticle beams have been introduced [29, 30]. Their general characteristics make them particularly suited for nanomaterial integration onto micromachined substrates, since they overcome many of the limitations affecting the deposition techniques described so far. The principle at the base of nanoparticle beam deposition (also cluster beam deposition, CBD) is the use of a carrier gas undergoing a supersonic expansion, as it moves from the

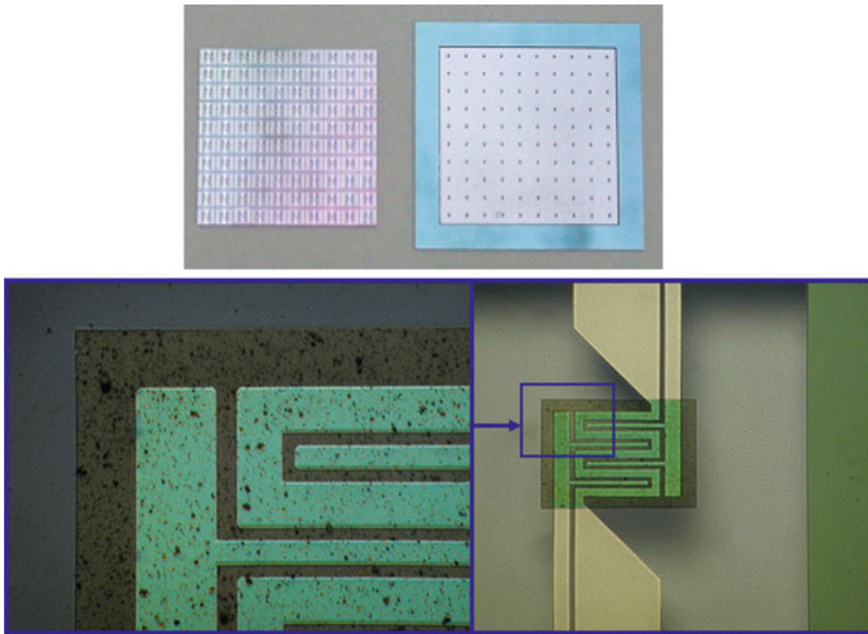

Fig. 16.14 *Top* image shows a wafer section hosting one hundred of microhotplates (*left*) and the micromachined auto-aligning silicon mask for non-contact patterning (*right*). Devices have been functionalized in batch with nanostructured WO_3 oxide, in a simple and straightforward step, by nanoparticle beam deposition, as shown in the *bottom* images. The active material is the *greenish rectangular* region on the interdigitated electrodes; it has dimensions of 0.65×0.78 mm^2. Reprinted from Ref. [31]

relatively high pressure condition of the beam source to the low pressure condition of a vacuum chamber, through a suitable nozzle, as shown in Fig. 16.11. The carrier gas, which is typically an inert gas, transports the nanoparticles, generated by bottom-up growth mechanisms and loaded into the gas stream, directly from beam source to deposition substrate, through a sequence of vacuum chambers. Once the nanoparticles reach the deposition chamber and substrate, they become the building blocks for the growth of nanostructured films. The entire process is performed at room temperature.

Although various type of nanoparticle beam sources exist, the pulsed microplasma cluster source (PMCS) appears to be one of the most promising for nanomaterial integration onto microhotplates for gas sensors. These promising attributes consist of the wide library of metal-oxides that it can produce, its stability, and the possibility of use it into large-scale production facilities.

Nanoparticle beams are characterized by low kinetic energy (fraction of eV per atom), which promotes a good adhesion as well as prevents nanoparticle destruction once they strike the substrate. Nanoparticle structure is preserved and their assembly during film growth leads to high specific surface area films which

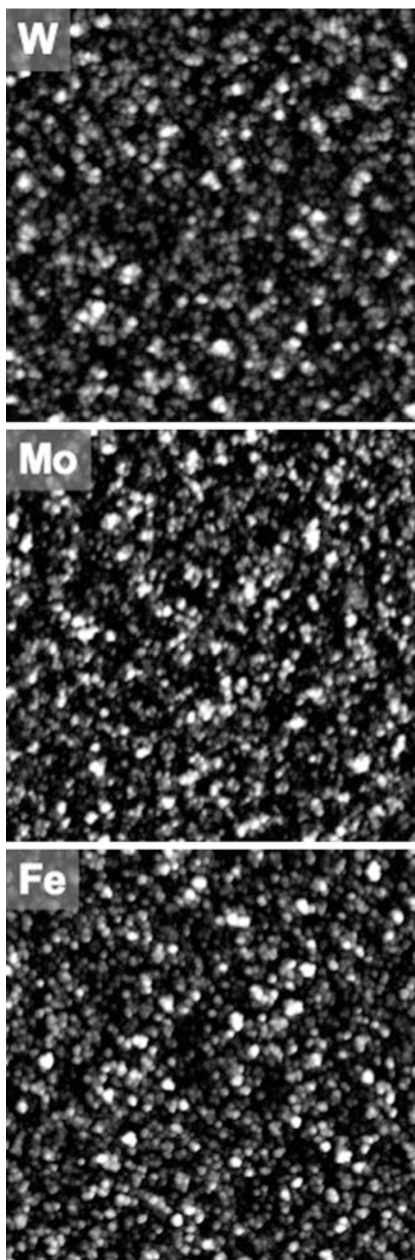

Fig. 16.15 Atomic force microscopy (*AFM*) images showing the surface morphology of films by nanoparticle beam deposition (the side of the images corresponds to 1 μm, while the thickness of the films is a few tens of nm). Morphological features are pretty much similar for all materials: this may be ascribed to ballistic regime growth, which is characterized by nanoscale porosity, poorly-connected and non-compact structures with lower density respect to bulk and a surface roughness increasing with film thickness. Reprinted from Ref. [33]

are very well suited for the interaction with the sampling atmosphere. Figure 16.12 shows an example of a film produced using nanoparticle beams.

The most relevant feature of nanoparticle beams, that strongly differentiate this technique from other gas-phase deposition techniques, is their high collimation,

which is of the order of few tens of mrad. Such a narrow beam leads to various consequences. For example, the deposition region can be separated from the nanoparticle production region via the adoption of differential vacuum chambers, in order to provide cleanest, ultra-high-vacuum (UHV) growth conditions. Nevertheless the most important consequence is by far the possibility of non-contact hard mask patterning with sub-micrometric lateral resolution. Thanks to beam collimation, in fact, the drawing of the mask is exactly reproduced on the substrate, as a stencil, even if the distance between the mask and substrate is of the order of several tenth of a millimeter or more. Hard mask patterned deposition of micrometric structures spreading over an area of several cm^2 has been reported in refs. [31, 32]; and an example of them is shown in Fig. 16.13.

As with other gas-phase deposition techniques, the nanoparticle beam technique matches the delicacy requirement for microhotplate functionalization: no heating or damage of the substrate occurs. Batch deposition of hundreds of devices within a wafer can be performed—even if the beam spot size is limited to a centimeter—through substrate rastering in front of the nanoparticle beam. Non-contact hard mask methods fulfills the requirement of a mechanically safe way to pattern nanomaterials onto delicate micromachined substrates. As an example, Fig. 16.14 shows a wafer cut containing one hundred microhotplates, each of which have been functionalized in batch mode with nanostructured tungsten oxide, in a simple and straightforward step, by nanoparticle beam deposition. A micromachined silicon mask with proper sectioning provided auto-alignment with the microhotplate devices.

In addition, several nanostructured metal-oxides, such as SnO_2, TiO_2, WO_3, Fe_2O_3, MoO_3, ZrO_2, HfO_2, NbO_x, ZnO, PdO_x, can be routinely produced by PMCS. Beside those usually used in state-of-the-art metal-oxide gas sensing, many others are available, with advantages from the point of view of an array approach to chemical sensing.

A non-trivial, intriguing feature of nanostructured metal-oxides by PMCS, regards their surface morphology, which is the same for all [33], as shown in Fig. 16.15. This may be ascribed to ballistic regime growth [34], which is characterized by nanoscale porosity, poorly-connected and non-compact structures, with lower density with respect to bulk and a surface roughness which increases with an increase in film thickness.

This rules out a common drawback realized with other deposition techniques. Mainly, the surface morphology (i.e. roughness, porosity, grain interconnection, etc.) may depend on the material produced, introducing an additional complexity element that makes it difficult to ascribe functional performances, such as gas sensing, to material chemistry rather than to a "convolution" between chemistry and surface micro- and nano- structure.

In summary, among the various deposition methods, nanoparticle beam deposition offers characteristic features, matching most of the requirements to be fulfilled for the integration of nanomaterials onto microhotplates and advanced micromachined platforms for chemical sensing: delicacy of deposition in itself; mechanically safe, non-contaminating, one-step method for micrometric patterning; batch deposition of hundreds of devices; several oxides with high specific surface available.

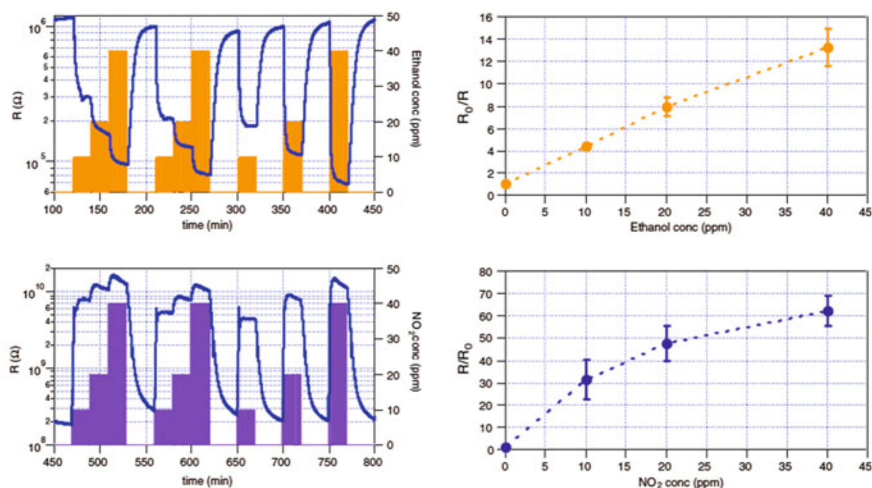

Fig. 16.16 Examples of sensing performances of microhotplates with nanoporous WO_3 by nanoparticle beam deposition, as active element. *Top* graphs show sensing results with respect to a reducing species, namely ethanol, while *bottom* graphs to an oxidizing species, namely NO_2. The operating temperatures are 300 °C for ethanol and 200 °C for NO_2, with a power of 24 and 13 mW, respectively. *Bar-like curves* indicate the nominal concentration of the test gases, referring to the *right axis*, while solid lines represent the resistance of the sensing film, referring to the *left axis*. Note that in both reducing and oxidizing cases, the use of the log scale for the *left axis* is required, due to the enormous change in sensor resistance. *Error bars* in response graphs on the *right* were calculated considering the three responses to the same gas concentration. Reprinted from Ref. [31]

16.4 Sensing Performances

16.4.1 Measurement Examples

The most important feature of microhotplate chemical sensors is by far the possibility to operate at high temperature spending a minimal amount of power. In addition, if their functionalization is done with high specific surface area porous nanomaterials, the sensitivity may be as high as to detect compound concentrations at ppb (parts per billion) levels. Figure 16.16 shows, as an example, the results of sensing characterization of microhotplates functionalized with nanostructured WO_3. In this case, the sensing material has been deposited, in the form of a nanoporous layer with a thickness of a few hundreds of nanometers, by nanoparticle beam deposition, using PMCS [31].

The Fig. 16.16 reports two examples of sensing performances relative to a reducing species (ethanol) and to an oxidizing one (nitrogen dioxide, NO_2). A decrease in resistance is observed upon exposure to a reducing gas, while an increase in resistance is observed upon exposure to an oxidizing gas. Resistance variations up to more than one order of magnitude were observed, at the injection

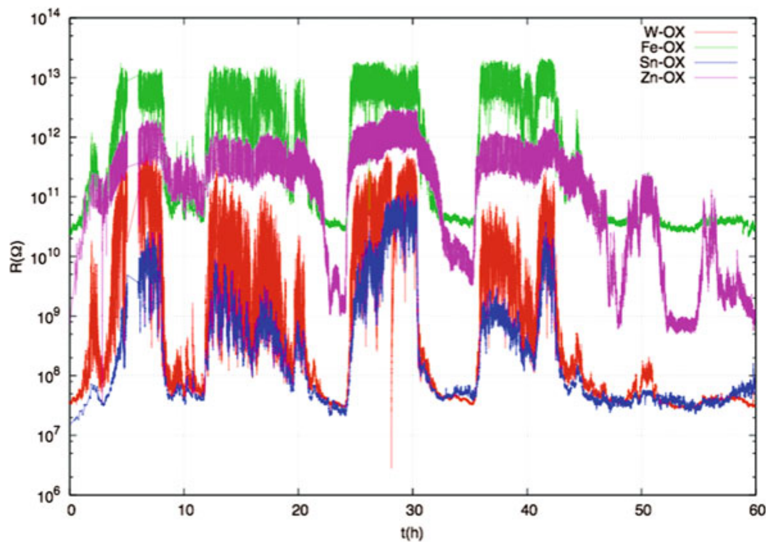

Fig. 16.17 Example of collective outputs of four nanostructured oxides (SnO_2, Fe_2O_3, WO_3 and ZnO) formed by nanoparticle beam deposition, exposed to the complex outdoor atmosphere of a car parking area. Although qualitatively similar, the sensing signals of different oxides are not identical each other: by means of advanced data analysis software with the capability of processing the collective response of the array, after suitable training it may be possible to recognize different chemical scenarios occurring in real outdoor atmosphere

of compounds with concentrations at ppm (parts per million) levels. Ethanol detection was carried out operating the microhotplate at a temperature of 300 °C, with a heating power of 24 mW, while NO_2 detection at 200 °C, with heating powers of 13 mW. Sensor responses, defined as R_0/R in the case of reducing species and R/R_0 for oxidizing species, R_0 being the sensor resistance in the presence of pure air only, and R the sensor resistance in the presence of the reactive compounds, were calculated and reported in Fig. 16.16 as well, as a function of the concentration of the test species. A saturation trend seems to appear at higher concentrations, while a good linearity is observed at lower ones, at ppm level. The strong response to NO_2 suggests a detection limit with respect to this compound in the 10–100 ppb range.

16.4.2 Microhotplate Array

A challenging problem of metal-oxide chemical sensing is the recognition of compounds, or at least their chemical family. In fact, due to the unspecific characteristics of the detection mechanism of chemoresistive sensors, different compounds at different concentrations may generate the same response in a single sensor. The strategy to try to address this issue passes through the use of sensor

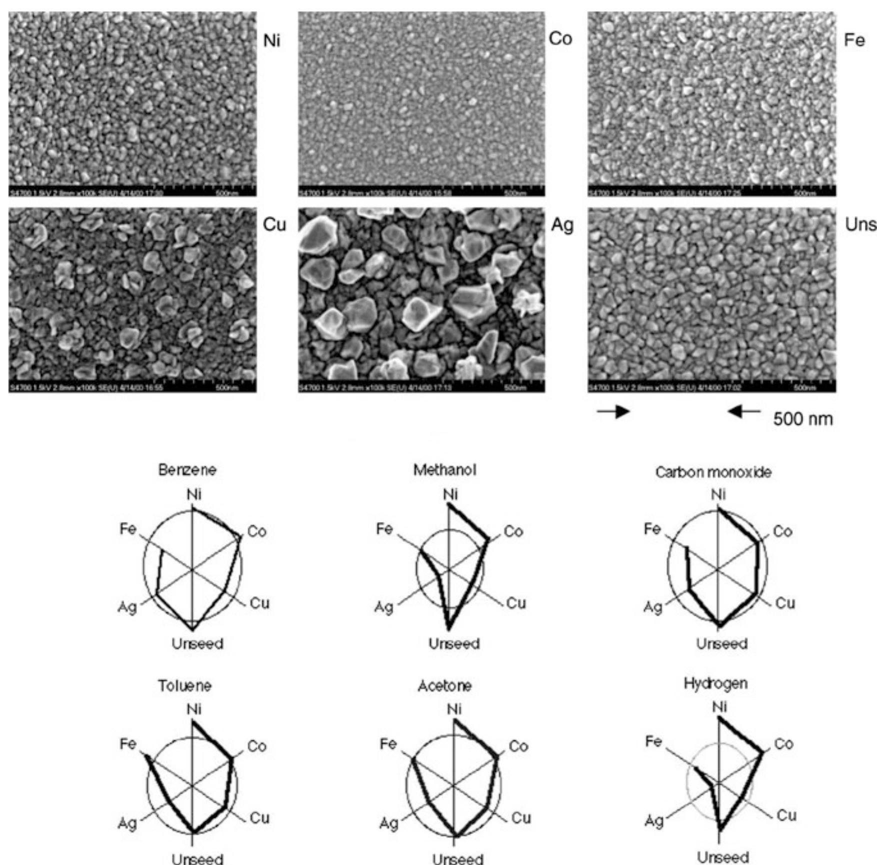

Fig. 16.18 In the *upper part* of the figure, SEM images showing the surface morphology of various sensing layers are reported. In all cases the sensing material is SnO_2 by CVD, however, the use of different metal seed layers before CVD process leads to different microstructures. *Bottom part* of the figure reports web-plots showing the relative sensitivity to six individual compounds in air of the sensing elements with an engineered microstructure. As in the case of Fig. 16.17, the use of an array of sensing materials may offer the possibility of compound recognition, although the intrinsic non-selectivity of metal-oxide chemical sensors. Reprinted from Ref. [3] with permission from Elsevier

arrays, where many sensors with different metal-oxides simultaneously react with the target chemical species. As an example of such a collective response, Fig. 16.17 shows the signals from four different nanostructured oxides deposited using a nanoparticle beam, namely SnO_2, Fe_2O_3, WO_3 and ZnO, during outdoor measurements.

Since the detection mechanism is generally the same for different oxides, sensor responses will be qualitatively similar, as clearly shown in Fig. 16.17. However, they are not identical. Hence, processing the collective response of the array, by means of advanced data analysis software (neural networks, for example),

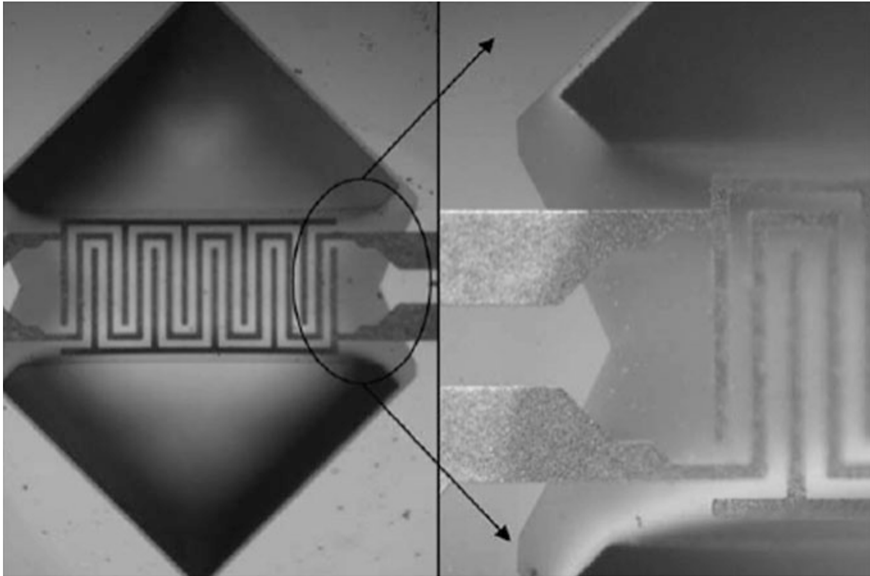

Fig. 16.19 Detail of suspended microbridge chemical sensor, within multiparametric platform. On the *left*, the entire suspended structure is visible, together with heater and interdigitated electrodes to contact the sensing layer. On the *right*, a close-up of the structure: the change of the color from *light* to *dark gray* along the *metal lines* indicates the border of the region deposited with nanostructured Fe_2O_3 by nanoparticle beam deposition. Reprinted from Ref. [36] with permission from Elsevier

precluded by a series of advanced training experiments against gases and gas mixtures of known composition, it may be possible to identify the "fingerprint" of the atmospheric gas composition.

Alternatives to arrays of different metal-oxides may be arrays of the same oxide having different microstructures, or different catalysts/dopants dispersed over the surface. In ref. [3] it is shown how the use of different metal seed layers before the deposition of SnO_2 by CVD, leads to different microstructures and to different relative sensitivities with respect to chemical compounds (Fig. 16.18).

16.4.3 Temperature Programmed Sensing

By exploiting the low thermal inertia of microhotplates, a temperature programmed sensing (TPS) mode can be adopted [35]. Analogously to array approach, the rationale at the base of TPS is the possibility to increase the data amount, by exploiting the different reactivity and different surface chemical processes in general, taking place at different temperatures, with the aim to improve

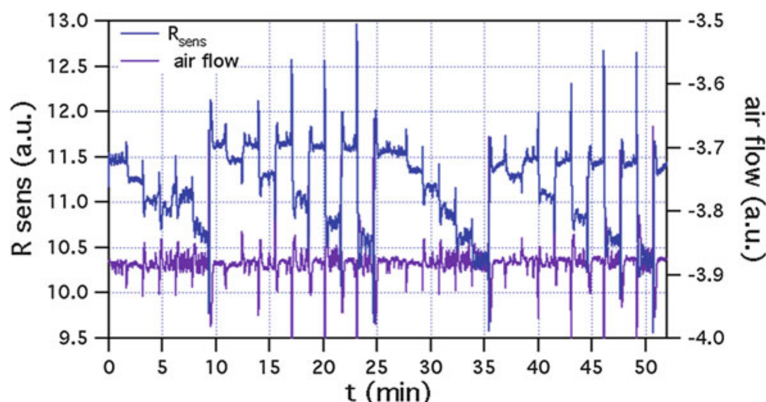

Fig. 16.20 Example of chemical sensing characterization of multiparametric device, with hydrogen in dry air at concentrations up to 30 ppm (*blue line*). The graph also reports the signal from micromachined anemometer, as a constant line with superimposed peaks (*violet line*). If the constant overall behavior of anemometric measure accounts for the constant total flow adopted—as usual—during chemical sensing experiment, superimposed peak-like features account for real fluctuations of air flow during MFCs operations, once hydrogen concentration has to be changed. Courtesy from L. Lorenzelli, FBK-Trento

the recognition capability of sensing systems with respect to complex atmospheres. The details of this methodology are highlighted in Chap. 14 in this book volume.

In an advanced approach to complex chemical sensing (as required for example to address security issues regarding the early detection of hazardous compounds such as chemical warfare agents), it is straightforward to merge together an array approach and TPS, in order to strongly increase the quantity of data characterization within a certain atmosphere [5].

16.4.4 Multiparametric Sensors

As shown in Sect. 16.2, microelectronic and micromachining methods for microhotplate production, are quite naturally extendible to include onto the same sensing platform other types of transducers, according to a common system integration approach. In particular, the example of a multiparametric platform hosting a chemical sensor, a thermometer, and an anemometer has been presented. Such a device may find applications as an in-line operating sensing system, with the capability to measure air flow and temperature, as well as to detect the presence of reactive compounds within flowing air. In a more specific example, these devices may find a role as novel miniaturized detectors, in charge of sampling the column outlet in advanced gas-chromatographic systems: feedbacks on column flow and outlet temperature, as well as, obviously, detection of chemical species, constitute the multiparametric task to be faced.

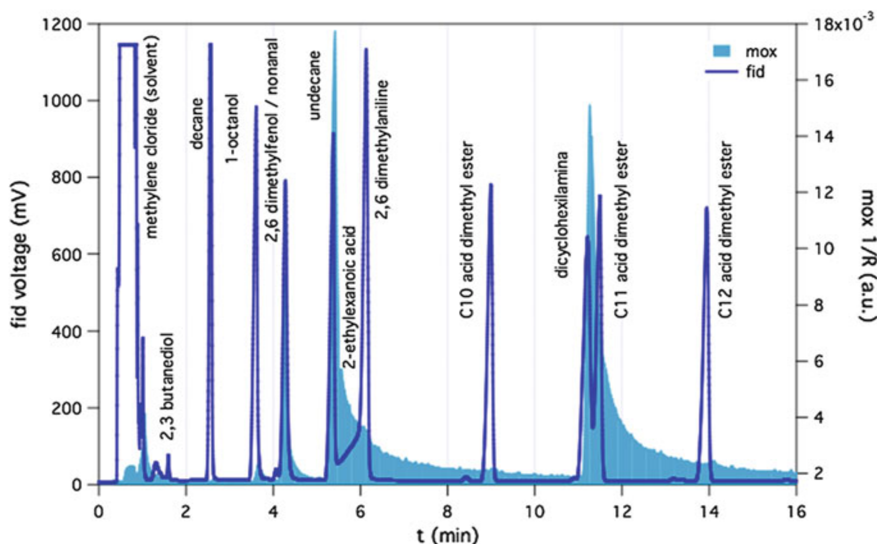

Fig. 16.21 Chromatogram acquired at the same time by a standard flame ionization detector (*FID*) and by the metal-oxide chemical sensor of a multiparametric micromachined platform. Not all the peaks visible with *FID* are detected also by metal-oxide sensor, which seems to be most sensitive to compounds containing hydroxyl group. Signal recovery after intense peaks shows long tails, probably due to inefficient atmosphere purging in the experimental setup, for gasdynamic reasons. Absence of sensitivity to the solvent (methylene chloride) could help in the detection of compounds with small retention time, or in the case of bad injections with solvent-modified baseline

Figure 16.19 shows a detail of the “microbridge” suspended structure of chemical sensor (see also bottom part of Fig. 16.8), which has been functionalized with nanostructured Fe_2O_3 by nanoparticle beam deposition [36]. Hard mask patterning limited the deposition of nanomaterial to chemical transducer only.

Platform characterization was carried out with a standard facility for gas sensor characterization, namely a test cell fluxed by means of mass flow controllers (MFCs) with the suitable atmosphere under investigation. Figure 16.20 shows an example of chemical sensing characterization with respect to hydrogen in dry air, at concentrations of 6, 12, 18, 24, and 30 ppm. Hydrogen injections correspond to descending square features of sensor resistance. On the same graph it is also reported the simultaneous signal from a micromachined anemometer: this is a constant line with superimposed upward and downward peaks. Constant behavior of anemometer signal indicates that chemical sensing characterization took place at constant total flow. Peaks are not simply signal noise: they account for real fluctuations of air flow during MFCs operations, once pure air flow is slightly decreased and hydrogen containing flow is increased to determine the proper hydrogen concentration, while maintaining constant the total flow over the device.

As an example of gas-chromatographic use of micromachined chemical sensor, Fig. 16.21 shows a chromatogram, which has been acquired at the same time from

a standard FID (hydrogen-fueled flame ionization detector) and from the multi-parametric device. Although not all the compounds can be revealed by the metal-oxide chemical transducer, as well as gas sensor design needs to be improved to enhance recovery time dynamics (in order to short peaks tails), gas-chromatographic use of advanced micromachined devices seems not so far fetched, at least within portable instrumentations and "first order" analysis, skipping the needs of a hydrogen line, as imposed by FID.

16.5 Conclusions and Perspectives

Advanced chemical sensors based on micromachined platforms integrating metal-oxide nanomaterials as active elements have high potentiality to address the demand of high-sensitivity, wide-spectrum, miniaturized, low power consumption, reliable and stable devices, to bridge the gap between current solid-state sensing technology and challenging, real-world applications. These include, for example, pervasive outdoor/indoor monitoring of air conditions through wireless sensor networks, early detection of hazardous compounds for security issues, food quality monitoring, etc. up to cutting edge applications such as physiological/pathological condition identification through breath analysis, or microclimatic characterization of artistic and cultural heritages sites for conservation purposes.

Beyond technical details, to make all this real, a novel vision is developing, where the concept of system integration, i.e. the synergistic contribution of the various technological aspects playing a role in the building and in the functionality of a complex system, constitutes the background scenario. This particularly holds for the issue of microhotplate functionalization with nanomaterials, where several techniques could be used, although so far none of them seems to be the optimal one, and in any case a careful merging of microelectronic production methods, micromachining methods, and nanomaterial production and integration methods has to be reached.

From this specific point of view, many of the techniques for the production of metal-oxide nanomaterials may be refined in their features to match requirements for large-scale, reliable, safe, cost-affordable integration of active layers on microhotplates and micromachined platforms. Among those techniques, nanoparticle beam deposition may be a novel tool with particular features making it suited for nanomaterial integration purposes. Gas-phase approach, non-contact hard mask patterning, batch deposition, as well as a wide library of synthesizable oxides with nanoporous structures, are its strength points.

From a more general point of view, the feeling is that parts composing metal-oxide advanced sensing systems, namely micromachined platform, active nanomaterial layer, device packaging, integrated electronics, wireless communication units, and advanced software for network and data managing, are all reaching a mature development stage. However, although the richness of lab-scale experiments, where testing is carried out with respect to several different atmospheres,

are claimed to reproduce real situations, a validation through long-term experiments at end-user sites, seems to be still lacking. This real-world validation is the next challenging frontier to be crossed.

References

1. Simon I, Bârsan N, Bauera M, Weimar U (2001) Micromachined metal oxide gas sensors: opportunities to improve sensor performance. Sens Actuators B 73:1–26
2. Briand D, Krauss A, van der Schoot B, Weimar U, Barsan N, Gopel W, de Rooij NF (2000) Design and fabrication of high-temperature micro-hotplates for drop-coated gas sensors. Sens Actuators B 68:223–233
3. Semancik S, Cavicchi RE, Wheeler MC, Tiffany JE, Poirier GE, Walton RM, Suehle JS, Panchapakesan B, DeVoe DL (2001) Microhotplate platforms for chemical sensor research. Sens Actuators B 77:579–591
4. Meijer G, Herwaarden A (1994) Thermal sensors, sensors series. Institute of Physics Publishing, Bristol and Philadelphia
5. Meier DC, Evju JK, Boger Z, Raman B, Benkstein KD, Martinez CJ, Montgomery CB, Semancik S (2007) The potential for and challenges of detecting chemical hazards with temperature-programmed microsensors. Sens Actuators B 121:282–294
6. Adami A, Lorenzelli L, Guarnieri V, Francioso L, Forleo A, Agnusdei G, Taurino AM, Zen M, Siciliano P (2006) A WO_3-based gas sensor array with linear temperature gradient for wine quality monitoring. Sens Actuators B 117:115–122
7. Raman B, Meier DC, Evju JK, Semancik S (2009) Designing and optimizing microsensor arrays for recognizing chemical hazards in complex environments. Sens Actuators B 137:617–629
8. Barsan N, Schweizer-Berberich M, Gopel W (1999) Fundamental and practical aspects in the design of nanoscaled SnO_2 gas sensors: a status report. J Anal Chem 365(4):287–304
9. Kohl D (2001) Function and applications of gas sensors. J Phys D Appl Phys 34:R125–R149
10. Ivanov P, Llobet E, Vergara A, Stankova M, Vilanova X, Hubalek J, Gracia I, Cané C, Correig X (2005) Towards a micro-system for monitoring ethylene in warehouses. Sens Actuators B 111–112:63–70
11. Afridi MY, Suehle JS, Zaghloul ME, Berning DW, Hefner AR, Cavicchi RE, Semancik S, Montgomery CB, Taylor CJ (2002) A monolithic CMOS microhotplate-based gas sensor system. IEEE Sens J 2(6):644–655
12. Graf M, Barrettino D, Zimmermann M, Hierlemann A, Baltes H, Hahn S, Bârsan N, Weimar U (2004) CMOS monolithic metal–oxide sensor system comprising a microhotplate and associated circuitry. IEEE Sens J 4(1):9–16
13. Suehle J, Cavicchi RE, Gaitan M, Semancik S (1993) Tin oxide gas sensor fabricated using C-MOS micro-hotplates and in situ processing. IEEE Electron Device Lett 14:118–120
14. Graf M, Gurlo A, Barsan N, Weimar U, Hierlemann A (2006) Microfabricated gas sensor systems with sensitive nanocrystalline metal-oxide films. J Nanopart Res 8:823–839
15. Su M, Li SY, Dravid VP (2003) Miniaturized chemical multiplexed sensor array. J Am Chem Soc 125:9930–9931
16. Vincenzi D, Butturi MA, Guidi V, Carotta MC, Martinelli G, Guarnieri V, Brida S, Margesin B, Giacomozzi F, Zen M, Pignatel GU, Vasiliev AA, Pisliakov AV (2001) Development of a low-power thick-film gas sensor deposited by screen-printing technique onto a micromachined hotplate. Sens Actuators B 77:95–99
17. Vincenzi D, Butturi MA, Stefancich M, Malagu C, Guidi V, Carotta MC, Martinelli G, Guarnieri V, Brida S, Margesin B, Giacomozzi F, Zen M, Vasiliev AA, Pisliakov AV (2001) Low-power thick-film gas sensor obtained by a combination of screen printing and micromachining techniques. Thin Solid Films 391:288–292

18. Riviere B, Viricelle JP, Pijolat C (2003) Development of tin oxide material by screen-printing technology for micromachined gas sensors. Sens Actuators B 93:531–537
19. Viricelle JP, Pijolat C, Riviere B, Rotureau D, Briand D, de Rooij NF (2006) Compatibility of screen-printing technology with micro-hotplate for gas sensor and solid oxide micro fuel cell development. Sens Actuators B 118:263–268
20. Jimenez I, Cirera A, Cornet A, Morante JR, Gracia I, Cané C (2002) Pulverisation method for active layer coating on microsystems. Sens Actuators B 84:78–82
21. Stankova M, Ivanov P, Llobet E, Brezmes J, Vilanova X, Gràcia I, Cané C, Hubalek J, Malysz K, Correig X (2004) Sputtered and screen-printed metal oxide-based integrated microsensor arrays for the quantitative analysis of gas mixtures. Sens Actuators B 103:23–30
22. Francioso L, Russo M, Taurino AM, Siciliano P (2006) Micrometric patterning process of sol–gel SnO_2, In_2O_3 and WO_3 thin film for gas sensing applications: towards silicon technology integration. Sens Actuators B 119:159–166
23. Smith DL (1995) Thin-film deposition: principles and practice. McGraw-Hill Professional, New York
24. Martin PM (2009) Handbook of deposition technologies for films and coatings: science, applications and technology. William Andrew—Elsevier, Oxford)
25. Chrisey DB, Hubler GK (1994) Pulsed laser deposition of thin films. Wiley-interscience, Hoboken New Jersey
26. Mattox DM (2010) Handbook of physical vapor deposition (PVD) processing. William Andrew—Elsevier, Oxford
27. Semancik S, Cavicchi RE (1991) The growth of thin, epitaxial SnO_2 films for gas sensing applications. Thin Solid Films 206:81–87
28. Cavicchi RE, Suehle JS, Kreider KG, Shomaker BL, Small JA, Gaitan M, Chaparala P (1995) Growth of SnO_2 films on micromachined hotplates. Appl Phys Lett 66:812–814
29. Milani P, Iannotta S (1999) Cluster beam synthesis of nanostructured materials. Springer, Berlin
30. Wegner K, Piseri P, Vahedi Tafreshi H, Milani P (2006) Cluster beam deposition: a tool for nanoscale science and technology. J Phys D 39:R439–R459
31. Barborini E, Vinati S, Leccardi M, Repetto P, Bertolini G, Rorato O, Lorenzelli L, Decarli M, Guarnieri V, Ducati C, Milani P (2008) Batch fabrication of metal oxide sensors on micro-hotplates. J Micromech Microeng 18:055015
32. Barborini E, Piseri P, Podestà A, Milani P (2000) Cluster beam microfabrication of patterns of three-dimensional nanostructured objects. Appl Phys Lett 77:1059–1061
33. Barborini E, Corbelli G, Bertolini G, Repetto P, Leccardi M, Vinati S, Milani P (2010) The influence of nanoscale morphology on the resistivity of cluster-assembled nanostructured metallic thin films. New J Phys 12:073001
34. Barabasi AL, Stanley HE (1995) Fractal concepts in surface growth. Cambridge University Press, Cambridge
35. Kunt TA, McAvoy TJ, Cavicchi RE, Semancik S (1998) Optimization of temperature programmed sensing for gas identification using micro-hotplate sensors. Sens Actuators B 53:24–43
36. Decarli M, Lorenzelli L, Guarnieri V, Barborini E, Vinati S, Ducati C, Milani P (2009) Integration of a technique for the deposition of nanostructured films with MEMS-based microfabrication technologies: application to micro gas sensors. Microelectron Eng 86: 1247–1249